Available online at www.sciencedirect.com
SCIENCE DIRECT
Polymer 45 (2004) 8791–8799
polymer
www.elsevier.com/locate/polymer

Structure and dynamics of a pentablock copolymer of polystyrene-polybutadiene in a butadiene-selective solvent

Huifen Nie[a], Minghai Li[a], Rama Bansil[a,*], Čestmír Koňák[b], Martin Helmstedt[c], Jyotsana Lal[d]

[a]*Center for Polymer Studies and Department of Physics, Boston University, Boston, MA 02215, USA*
[b]*Institute of Macromolecular Chemistry, Academy of Sciences of the Czech Republic, Heyrovsky Sq. 2, 162 06 Prague 6, Czech Republic*
[c]*Fakultät für Physik und Geowissenschaften, Universität Leipzig, Linnestrasse 5, D-04103 Leipzig, Germany*
[d]*Argonne National Laboratory, Argonne, IL 60439, USA*

Received 25 May 2004; received in revised form 18 October 2004; accepted 19 October 2004

Abstract

We have examined solutions of a polystyrene-polybutadiene pentablock copolymer in *n*-heptane, a strongly selective solvent for polybutadiene. Small angle neutron scattering from 7 to 15% samples reveals domains about 10 nm in radius formed by the association of ~200 polystyrene blocks. Dynamic light scattering measurements on 8 and 9% samples showed three modes: a fast diffusive mode related to the collective diffusion in semidilute solutions/gels; a relaxational mode related to the local dynamics of polystyrene domains trapped in the gel formed by bridging the domains with the polybutadiene chains; and a very slow diffusive mode. The relaxational dynamics persisted over the entire temperature range, becoming faster with increasing temperature, indicating a decreased microviscosity at higher temperatures. The slow dynamics seems to be connected with heterogeneities in the physical gel due to microsyneresis and almost disappeared above 50 °C. Macroscopic phase separation into two liquid phases was observed in a dilute solution of the un-associated copolymer, and into a liquid and gel phase at higher concentrations. The absence of flower-like micelles in dilute solutions and the macroscopic phase seperation suggest that the gels in the pentablock are formed by random association of multiplet domains and not by bridging of micellar domains.

Keywords: Dynamic light scattering; Neutron scattering; Multiblock copolymer

1. Introduction

Micellization of diblock copolymers in selective solvents has been extensively investigated [1–3], and it is well known that core-shell micellar particles are formed in diblock solutions in a solvent selective for either block at concentrations above the critical micellar concentration (cmc) and below the critical micellar temperature (cmt). Studies of diblocks in solvents of varying selectivity have shown the interplay of solvent–polymer interactions and polymer–polymer interactions in controlling the phase behavior and morphology of ordered phases [4–5]. In the case of tri- and higher multiblocks the competition between looping and bridging of the soluble chains, and factors related to end-block versus inner block solubility further complicate the issue. Thus in ABA triblock copolymers the solvent selectivity determines whether isolated micelles will form (solvent selective for the outer block, A) or flower-like micelles or bridged micellar networks (solvent selective for the middle block, B) depending on the relative contributions of loops versus bridges to the free energy [6–13]. For copolymers with more than three blocks, e.g. $(AB)_n$ multiblocks with $n \geq 2$, bridged structures are expected to form irrespective of which block the solvent prefers. Several groups have shown that the insoluble poly A blocks in the triblock systems can be approximated by spherical cores [8, 14,15] giving rise to gels which consist of bridged micellar networks. For higher multiblocks the presence of multiple bridges gives rise to physical gels similar to those formed by the association of ionomers [16] in that the insoluble A blocks of the multiblock copolymer form multiplet-like nodes, i.e cross-links, connected by the soluble B chains. This tendency of the insoluble blocks to associate leads to

* Corresponding author. Tel.: +1 617 353 2969; fax: +1 617 353 9393.
E-mail address: rb@bu.edu (R. Bansil).

0032-3861/$ - see front matter © 2004 Published by Elsevier Ltd.
doi:10.1016/j.polymer.2004.10.051

the formation of polydisperse clusters at low copolymer concentrations eventually forming a gel above some critical concentration [16,17]. In contrast to micellization which is described by a 'closed association' model [see Ref. [1] for definition] with a single equilibrium constant and a cmc, the aggregation of ionomers and multiblocks is likely to be controlled by a series of equilibria between single, contracted chains and multi-chain clusters described by the 'open association' model [1,17]. Computer simulations of multiblock copolymer solutions also predict a variety of isolated and bridged network-like structures [18].

The rich phase behavior and physical gelation of multiblock coplymers in selective solvents has numerous practical applications. From a fundamental view-point the systematic evaluation of relations between multiblock copolymer structure and properties of selective solvents on one hand and properties of the gels formed by them on the other hand is valuable to understanding the behavior of ordered physical gels formed by solvent-mediated random association in multiblock copolymers in selective solvents.

To address the association behavior, we have previously examined the pentablock copolymer, SBSBS of polystyrene (PS) and polybutadiene (PB) in 1,4-dioxane (a good solvent for PS and a theta solvent for PB) by small angle neutron scattering (SANS) and dynamic light scattering (DLS) [19]. No flower-like micelles were found in dilute solutions. The SANS data at 25 °C clearly revealed interacting domains, approximately 6 nm in radius, formed by association of the insoluble PS block in the 20% sample. The 4% sample did not show such domains, while that at 7% represented an intermediate situation, with both unassociated polymer and associated polymer. At higher temperatures the domains dissolved. The DLS data for samples with concentration of 2–22% exhibited two diffusive modes, a fast mode corresponding to cooperative dynamics of concentration fluctuations and a slow mode to the diffusion of the large length scale heterogeneities. The strong angular dependence of the static light scattering (SLS) implies that small micro-domains of about 10–15 PB blocks are bridged by the PS chains forming large aggregates with randomly distributed crosslinks on length scales much larger than the domain size. Gelation was not observed in any of the dioxane samples, reflecting the weak association behavior in a theta solvent like dioxane. In this paper, we continue this research by examining the same pentablock copolymer in heptane which is a strongly selective solvent for the butadiene blocks. The two solvents also differ in another important way; in dioxane the outer PS blocks of the pentablock are in a good solvent environment whereas in heptane they are in a poor solvent environment. This might further promote cross-linking. The SANS and DLS measurements in dilute and semidilute concentration regime over a range of temperatures are compared with those from a similar triblock in heptane as well as from the pentablock in dioxane in an effort to understand the influence of varying solvent selectivity and number of blocks on the association behavior of multiblock copolymers.

2. Experimental

2.1. Copolymer

A pentablock copolymer, poly(styrene-*block*-butadiene-*block*-styrene-*block*-butadiene-*block*-styrene) SBSBS (Kaučuk Kralupy, Kralupy, CZ), was fractionated to reduce content of residual homopolymers and diblock copolymers. No trace of unreacted homopolymer was found in GPC distributions after the fractionation. The molecular weight of the sample was $M_w = 1.2 \times 10^5$ g/mole (light scattering in tetrahydrofuran), polydispersity $M_w/M_n = 1.10$ (GPC) and mass fraction of styrene was 0.35 (NMR). According to the manufacturer's specification M_n of the butadiene (B) blocks is 3.2×10^4 g/mole, that of the outer styrene blocks is 1.3×10^4 g/mole and of the middle styrene block 9×10^3 g/mole.

2.2. Solutions

Dust-free semidilute solutions for light scattering measurements were prepared from a 2 wt% solution in cyclopentane (a good solvent for the copolymer at 25 °C) directly in the dust-free cylindrical optical cells and the cyclopentane was then removed by evaporation in vacuum at room temperature. The weights of samples were checked during the evaporation process to ensure complete removal of the cyclopentane. For samples of higher concentrations, the procedure was repeated until the desired amount of the copolymer was accumulated in the cell. The required amount of the filtered selective solvent, *n*-heptane, was then added and cells were sealed. The dissolution of the copolymer of higher concentrations took several hours at 65 °C. For neutron scattering measurements solutions of the pentablock copolymer were prepared by direct dissolution in deuterated *n*-heptane at 65 °C until a clear solution was formed. The samples were stabilized by an inhibitor (0.5 wt% of the copolymer content) octadecyl 3-(3,5 ditert.butyl-4-hydroxyphenyl) propionate (Irganox 1076). All concentrations are given as percentages (w/v).

2.3. Dynamic light scattering

Polarized DLS measurements were made in the scattering angle range of 30–135° using a light scattering apparatus equipped with an solid state laser ($\lambda = 532$ nm) and an ALV 5000, multi-tau autocorrelator covering approximately 11 decades in delay time t. Because a wide distribution, $A(\tau)$, of decay times, τ, is expected, the correlation functions were analyzed with the program REPES [20], to determine the inverse Laplace transform of the electric field correlation function, $g^{(1)}(t)$

$$g^{(1)}(t) = \int A(\tau)\exp(-t/\tau)\mathrm{d}\tau, \quad (1)$$

The program REPES is similar to the widely used program CONTIN [21], except that it actually inverts the measured intensity correlation function $g^{(2)}(t) = 1 + C|g^{(1)}(t)|^2$, where C is an instrumental constant.

Since the REPES analysis has a tendency to overfit, thus splitting broad distributions into two or more contributions, the electric field autocorrelation functions, $g^{(1)}(t)$, were also fitted to a sum of one or two single exponentials and a stretched exponential function:

$$g^{(1)}(t) = A_o + A_1 \exp(-[t/\tau_1]) + A_2 \exp(-[t/\tau_2]^{\beta}) + A_3 \exp(-[t/\tau_3]), \quad (2)$$

where τ_i are characteristic decay times, A_i relative scattering amplitudes; $\sum A_i = 1$. The exponent $\beta(0 \le \beta \le 1)$ is a measure of the width of the corresponding distribution of the relaxation times τ; the smaller the value of β, the broader is the distribution. The DLS results are presented throughout the paper using the normalized intensity autocorrelation functions, $g^{(2)}(t)$.

The mean relaxation time, τ_{2w}, of the stretched exponential mode is given by

$$\tau_{2w} \equiv (\tau_2/\beta)\Gamma(1/\beta), \quad (3)$$

where $\Gamma(1/\beta)$ is the gamma function. The characteristic decay rates Γ_i are reciprocal values of τ_1, τ_3 and τ_{2w}. The hydrodynamic correlation length ξ_h was calculated by standard procedure using the Stokes–Einstein relation.

2.4. Static light scattering

Static light scattering measurements were performed with a Sofica instrument equipped with a vertically polarized He–Ne laser ($\lambda = 632.8$ nm) in the angular range of 30–150°. The processed data are represented (unless otherwise noted) as

$$Kc_t/\Delta R(\theta, c) = (M_w)^{-1} + 2A_2c_t, \quad (4)$$

where M_w is the weight-average molecular weight, K is the optical constant which includes the square of the refractive index increment $\mathrm{d}n/\mathrm{d}c$, $\Delta R(\theta)$ is the Rayleigh ratio, proportional to the excess intensity of light scattered from solutions as compared to the pure solvent, A_2 is the second virial coefficient, and c is the copolymer concentration in g ml^{-1}. The apparent weight-average molecular weight M_w^a was calculated from zero-angle limits of $\Delta R(\theta, c)/Kc = M_w^a$.

2.5. Small angle neutron scattering

Neutron scattering experiments were conducted at the Small-Angle Neutron Diffractometer (SAD) at IPNS, Argonne National Laboratory. Incident neutrons with wavelengths 0.9–14 Å were used in a time-of-flight instrument [22] with a two-dimensional detector to cover the scattering vector range $q = 0.005$–0.35 Å^{-1}. The SANS measurements were made in custom designed cells consisting of a cylindrical steel barrel fitted with quartz cells consisting of two quartz disks with a Teflon spacer with a path length of 1 mm maintained at a constant temperature. The isotropic two-dimensional scattering spectra were azimuthally averaged to obtain the scattered intensity $I(q)$ versus the magnitude of the scattering vector, q. The data were corrected for sample absorption, pure solvent background subtraction, and normalized to absolute beam intensity. All SANS data were converted to absolute intensity using calibration relative to a standard sample as described in Ref. [22].

2.6. SANS data analysis: model form factors and structure factor

For the analysis of the SANS data, we use the same model as in our previous work on the pentablock in dioxane [19] and triblock in selective solvents [13]. Briefly, we treat the scattering as arising from the sum of the contributions from the domains of the insoluble PS block and the swollen chains of the soluble block, and treat the PS domains as spherical cores of radius R_c. The interaction between cores is mediated both by the interpenetrating and bridged PB chains and the hard sphere repulsion of the PS cores. This interaction is characterized by a 'hard sphere' interaction radius R_{hs} which is larger than R_c and denotes the effective interaction radius of the hard sphere potential and is described by the Percus–Yevick structure factor. For details see Ref. [23]. To include the contribution to the SANS scattering intensity from the swollen PS chains we add a Lorentzian $S(q) = S_0/(1 + q^2\xi^2)$, with ξ representing the correlation length for concentration fluctuations due to polymer chains in the semidilute regime. Any scattering from unassociated polymer also contributes to the Lorentzian term.

The data were fit to the model described above using four parameters, I_0, R_c, R_{hs}, ϕ to describe the interacting hard spheres contribution to the scattering and two parameters, S_0 and ξ, to model the scattering due to concentration fluctuations of the polymer chains. The fitting was done using the nonlinear least squares program of Origin™. The parameters R_c and R_{hs} can be directly estimated from the minimum of the form factor and the position of the primary peak, as described in Ref. [13]. It is of course important to note that other schemes of fitting the data may also work; however, in this paper we restrict ourselves to the model discussed above as a means of quantifying structural changes. Polydispersity effects can be taken into account by adding, e.g. a Gaussian distribution of core sizes. We have not included this in order to keep the number of parameters to a minimum.

3. Results and discussion

3.1. Macroscopic phase behavior of the pentablock in n-heptane

The copolymer exhibited a limited range of solubility in *n*-heptane. In dilute solutions ($c<1\%$) it was not soluble in *n*-heptane at room temperature but it was possible to dissolve it at temperatures higher than 60 °C. On cooling, a macroscopic phase separation was observed with a cloud point about 57 °C for the copolymer with concentration $c=0.5\%$. No flower-like micelles were observed above the cloud point, in contrast to the behavior of the similar triblock, S-EB-S (Kraton G 1650, which has comparable overall molecular weight and molecular weight of the PS blocks and similar styrene fraction) in heptane. The reason for the difference could be partly in shorter butadiene blocks in the pentablock as compared to the EB block of the triblock and mainly (as we suppose), in the pentablock architecture. Two free-energy consuming loops of copolymer chain would be necessary to build the pentablock into a flower-like micelle as opposed to only one in the case of the triblock. Temperature dependence of the zero-angle normalized scattering intensity $Kc/\Delta R(0)$ and hydrodynamic correlation length ξ_h, as obtained from static and dynamic light scattering experiments, are shown in Fig. 1a and b, respectively. The results reveal strong increase in concentration fluctuations behavior in the vicinity of the phase separation temperature at 57 °C. Thus, SBSBS copolymer in dilute *n*-heptane solutions behaves similar to homopolymers with an average χ-parameter (like statistical copolymers) in thermodynamically poor solvent exhibiting a phase separation at low temperatures.

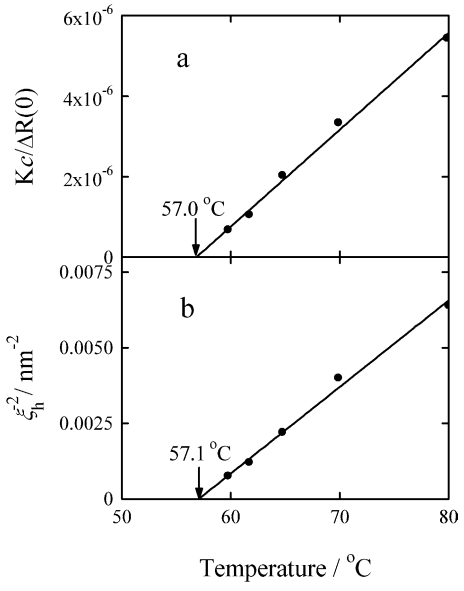

Fig. 1. Temperature dependence of the zero-angle normalized static light scattering intensity $Kc/\Delta R(0)$ (a) and hydrodynamic correlation length ξ_h (b) for dilute solution ($c=0.5\%$) of the pentablock in *n*-heptane.

Macroscopic phase separation was also observed at higher copolymer concentrations. Turbid samples with high viscosity were obtained at concentrations $c=2,4,6\%$. The turbidity of the samples due to microsyneresis was very high (multiple light scattering occurred), which made light scattering experiments impossible. These samples were not stable and over several days split into two phases, a liquid phase and a transparent gel phase with the equilibrium gel concentration $c_e=7.5\pm0.2\%$. The samples with concentration $c=8$ and 9%, which are close to c_e, were optically transparent so that dynamic light scattering measurements were possible. The viscosity of the samples was very high at room temperature, about 440 and 1090 Pa s for solutions with 8 and 9%, respectively. The samples with $c>9\%$ were also turbid at room temperature.

The phase behavior of the SBSBS pentablock in *n*-heptane is similar to that observed in physical gels such as gelatin under poor solvent conditions [24], where depending on the temperature and composition of the gel it is possible to either have complete macroscopic liquid–liquid, or liquid–gel phase separation, or to produce microphase separated gels.

3.2. Small angle neutron scattering

SANS measurements on 7, 8 and 15% solutions of the pentablock SBSBS in deuterated-heptane over the temperature range from 40 to 80 °C showed a well-defined peak whose intensity increases with decreasing temperatures. Such a peak is the hallmark of interacting domains or cores of the insoluble PS blocks. Typical data for the 8 and 15% samples are shown in Fig. 2. Decreasing concentration broadens the peak and reduces its intensity, but does not abolish the peak in this concentration range. In contrast, as shown in the inset of Fig. 2, the peak is absent in a 7% solution of the same pentablock in dioxane [19], reflecting stronger association in heptane as compared to dioxane.

3.2.1. Structural parameters from Percus–Yevick analysis

The results of fitting with the Percus–Yevick model of interacting hard spheres together with a Lorentzian term representing the scattering from concentration fluctuations at high q, are shown in Table 1 and the fits are shown in Fig. 2. The fit works well in the region of the primary peak, and the fitted values of R_c and R_{hs} are in excellent agreement with the estimates obtained from the minimum of the form factor and the position of the primary peak. However, the fit gives a more pronounced second order peak than is observed in the data. Similar discrepancy was observed by Kinning et al., [23] in the fit to a diblock copolymer. Presumably this reflects the effects of polydispersity and attractive interactions due to bridging, which are left out in the model. All of the parameters of the interacting hard spheres model decrease with increasing temperature indicating melting of the structure on heating. The volume fraction of cores is larger at higher concentration and the correlation length

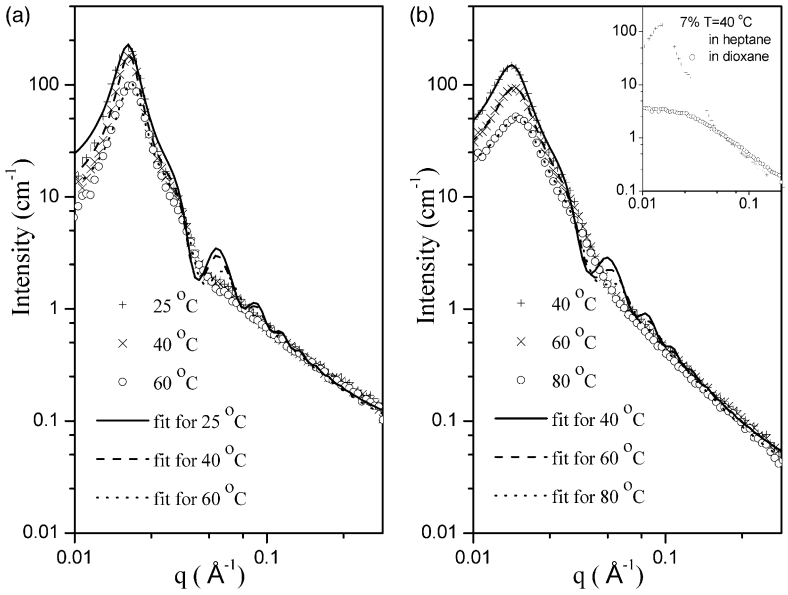

Fig. 2. SANS scattering from 15% (a) and 8% (b) solutions of the pentablock in *n*-heptane at different temperatures as indicated. The lines show the fit to the PY model with the Lorentzian term. In the inset the scattering from a 7% solution of the pentablock in dioxane [19] is compared to that of the 7% solution in *n*-heptane.

decreases with increasing concentration, as expected. With decreasing concentration the relative contribution of the Lorentzian part increases, reflecting the well-known increase in concentration fluctuations with decreasing concentration in the semi-dilute regime.

Since the cores of 15% sample at all the measurement temperatures give rise to a well defined scattering peak, we calculate an upper limit to the aggregation number N_{agg} (defined as the number of the insoluble PS blocks in the core) assuming that there is no solvent in the core. Thus $4/3\pi R_c^3 = N_{agg} V_{PS}$, and estimating the volume of the PS block from its molecular weight (M_{PS}) and density (ρ_{PS}), $V_{PS} = M_{PS}/N_A \rho_{PS} = 20.5\ nm^3$, we obtain $N_{agg} = 230$, 223 and 175 at 25, 40 and 60 °C, respectively. Previous studies indicate that about 30 vol% of the solvent would be present in the micro-domains at room temperature [25]. Thus, the aggregation numbers should be reduced approximately by 30%. The decrease in the aggregation number with increasing temperature is consistent with the decreasing tendency to associate at higher temperatures.

A comparison of the core radius of about 10 nm with L_{PS}, the end-to-end length of the outer PS blocks suggests that the PS chains are more stretched than Gaussian chains. (For the Gaussian chain $L_{PS} = a_{PS} N_{PS}^{0.5} = 7.9$ nm using $a_{PS} = 0.71$ nm. Here $N_{PS} \sim 125$ denotes the number of monomers in the outer PS block). This result is in agreement with the calculations of Nrkova et al., [16] on the association of multiblock copolymer melts. The core radius is closer to the end-to-end distance of self-avoiding walk chain, $L_{PS} = a_{PS} N_{PS}^{0.6} = 12.5$ nm. The PS stretching could be due to the pulling force of soluble PB blocks and/or the presence of solvent in the cores. Similarly, simple geometrical conditions imply that the end-to-end length of the chain which bridges two neighboring cores ($2(R_{hs} - R_c)$) is about 14 nm for both the solutions at 25 °C. This distance is comparable to the Gaussian chain length of the PB block ($L_{PB} = a_{PB} N_{PB}^{0.5} = 16.5$ nm using $a_{PB} = 0.68$ nm and $N_{PB} = 592$ the number of monomers in the PB block).

3.3. Dynamic light scattering

As shown in Fig. 3a, the intensity autocorrelation

Table 1
The parameters obtained by fitting a combination of Percus–Yevick and Lorentzian models to SANS experiments on the pentablock in *n*-heptane at different concentrations (c) and temperatures (T)

c (g ml^{-1})	T (°C)	R_c (nm)	R_{hs} (nm)	ϕ	I_{PY}	ξ (nm)	S_0
0.15	25	10.4	17.3	0.40	252.8±0.3	2.0	3
	40	10.3	17.3	0.43	191.8±5.5	2.0	3
	60	9.5	16.8	0.39	108.2±3.4	2.0	3
0.08	40	11.3	19.5	0.32	183.5±0.7	4.1	7.5
	60	10.8	18.7	0.31	115.6±0.8	4.1	7.5
	80	10.2	17.6	0.28	62.4±0.8	4.1	7.3

As defined in the text R_c denotes the core radius, R_{hs} the interaction radius, ϕ the hard sphere volume fraction and I_{PY} the peak intensity of the Percus–Yevick contribution to the scattering. The parameters ξ and S_0 correspond to the correlation length and zero-angle intensity of the Lorentzian term.

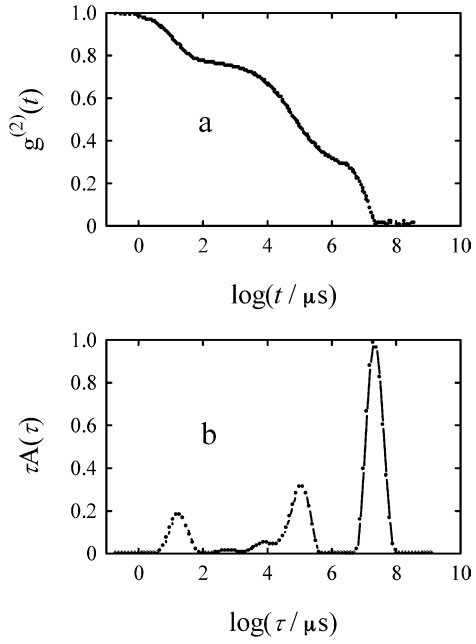

Fig. 3. (a) Normalized intensity autocorrelation function, $g^{(2)}(t)$, for a *n*-heptane solution of the pentablock ($c=8\%$) measured at the scattering angle of 90° and temperature of 25 °C. (b) Distribution, $A(\tau)$, of decay times, τ, obtained from REPES analysis of $g^{(2)}(t)$ shown above in (a).

function, $g^{(2)}(t)$ for an 8% solution at 25 °C is broad, extending over several orders of magnitude of delay time, t. Three dynamic processes can be extracted from the distributions of relaxation times using the REPES analysis of the correlation function as shown in Fig. 3b. Both the sharp peaks at short and long decay times can be related to single exponential decay in the correlation function, whereas the middle mode can be well approximated by a stretched exponential decay. Therefore, a fit to two single exponential functions and one stretched exponential function was used for the analysis of the correlation functions. The dependence of the characteristic decay rates of the three dynamic processes (Γ_i, $i=1$–3) on the scattering vector's magnitude, q is shown in Fig. 4 for the solution with $c=8\%$.

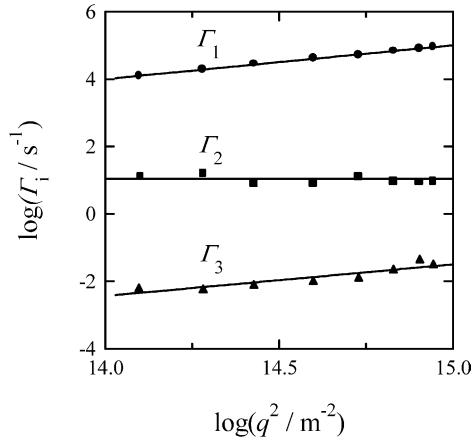

Fig. 4. The q^2-dependence of the decay rates, $\log \Gamma_i$ ($i=1$–3) vs $\log q^2$, for copolymer solutions with $c=8\%$ at 25 °C. The slow mode Γ_3 could not be detected above 50 °C.

While the fast and slow mode were found to be diffusive ($\Gamma_i \propto q^2$) the middle mode is relaxational, i.e. independent of q^2 in the measuring range. Similar behavior was observed for the sample with $c=9\%$. A small concentration dependence of Γ_i between samples with $c=8$ and 9% is observed as shown in Table 2 where zero-angle limits of Γ_i are shown for both the samples.

The DLS results observed for the pentablock in *n*-heptane have considerable similarity with results obtained for semidilute solutions/gels of S-EB-S triblock copolymer (Shell products, Kraton G-1650) in *n*-heptane [26,27]. In view of this we follow the same interpretation, relating the fast mode to the collective gel mode, the middle mode to the relaxational dynamics of the insoluble domains or multiplets which act as the crosslinks of the physical gel, and the slow mode to large length scale inhomogeneities.

By combining the light scattering and SANS data we can draw some simple conclusions about the length scales involved in the relaxational motion. First, the radius of the nodes or the object undergoing relaxational dynamics is comparable to the core radius, i.e. about 10 nm. Second, relaxational behavior can be observed when $1/q$ (30–100 nm in our experiment) is comparable or larger than the mean size of the gel pores [28]. To test the validity of this criterion we estimate the average pore size as comparable to the average interaction distance between two neighboring multilplet domains, $2R_{hs}$. From the SANS measurements we obtain a value of about 32 nm (see Table 1) which is comparable to the lowest $1/q$ in our experiment. It is important to clarify that these are crude estimates since the gel will have a distribution of pore-sizes.

3.3.1. Temperature dependence of the dynamics

To understand this complex dynamics we made DLS measurements at several temperature up to 65 °C. The temperature dependence of the decay rates Γ_i ($i=1$–3) from DLS measurements at a scattering angle of 90° for copolymer solution with $c=8\%$ is shown in Fig. 5a.

3.3.2. Collective diffusion and relaxational dynamics in the gel

The small increase in the decay rate of the fast collective diffusion mode, Γ_1 reflects the viscosity changes of *n*-heptane and the slight temperature dependence of the hydrodynamic correlation length (see Table 2). In contrast the relaxation rate of middle mode, Γ_2, increases more than three orders of magnitude on heating approaching Γ_1 at higher temperatures. Presumably this correlates with the decreased microviscosity of the gel as the volume fraction of the domains of the insoluble blocks decrease with increasing temperature, i.e. there are fewer crosslinks at higher temperatures (see Fig. 2 and Table 1). Furthermore, the slight decrease in the core radius with increase temperature would also lead to a faster relaxation rate.

Table 2
Dynamic parameters of the pentablock solution in *n*-heptane at different temperatures and concentration

T (°C)	c (g ml^{-1})	ξ_h (nm)	Γ_1 ($\times 10^3$ s^{-1})	Γ_2 (s^{-1})	Γ_3 (s^{-1})	fr_2	β
25	0.06[a]	24.5	12.3	7.85	–	0.78	0.62
	0.08	23.9	12.6	9.14	0.00447	0.70	0.63
	0.08[b]	23.3	12.9	8.91	–	0.73	0.63
	0.09	20.8	14.5	9.55	0.00275	0.72	0.58
35	0.08	30.4	11.0	84.7	0.0295	0.69	0.64
	0.09	19.2	17.4	109.6	–	0.66	0.59

The parameters are as described in the text.
[a] Gel phase after 6 months.
[b] After 6 months.

However, the middle mode remains relaxational over the entire temperature range examined in this study. The relative contribution of the relaxational mode to the sum of the two gel modes, fr_2 (defined as $A_2/(A_1+A_2)$) and the exponent β characterizing the polydispersity of the distribution of characteristic relaxation times, $A(\tau)$, of the middle mode are almost independent of temperature (see Fig. 5b). This observation is consistent with the SANS data which shows that the interacting domains persist at the highest temperature investigated. In this regard the pentablock domains are more stable than in the tri-block where a transition from relaxational to diffusive behavior of the middle mode was observed at high temperatures [26,27].

3.3.3. Slow mode and phase separation

The slowest mode which is diffusive is the most complicated to interpret. The origin of this mode is not fully understood, it may reflect the heterogeneity inherent in a block copolymer due to the existence of two or more monomers; or it may represent an association between chains. Slow modes, called cluster-modes have been observed in the long-range density correlations of homopolymer and copolymer melts and low molecular weight glass formers [29–32]. In physical gels such as those used here microsyneresis is commonly observed and would give rise to long-length scale inhomogeneities. We suggest that this is most likely cause of the slow mode seen in the pentablock samples. This interpretation of the slow mode is supported by the strong temperature dependence of Γ_3 as shown in Fig. 5a and the pronounced decrease in the relative scattering intensity, A_3 of the slow mode on heating. The slow mode cannot be detected at 50 °C and higher temperatures suggesting that microsyneresis becomes weaker with increasing temperature.

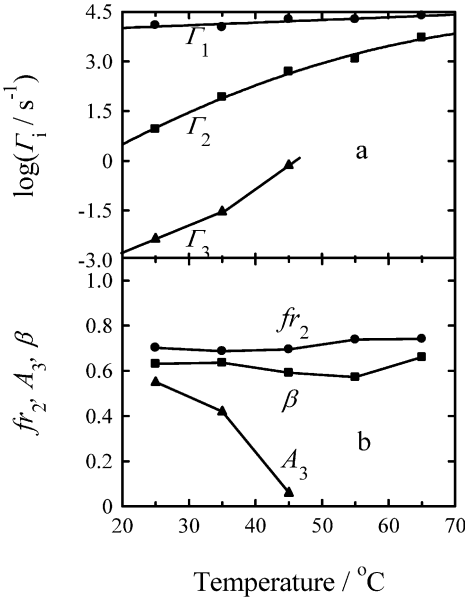

Fig. 5. (a) Temperature dependence of log Γ_i ($i=1$–3) for 8% copolymer solution obtained from normalized intensity autocorrelation functions measured at $\theta=90°$. (b) The temperature dependence of the contribution of the relaxational mode relative to the sum of the two gel modes, fr_2, the exponent β of the relaxational mode, and the relative scattering intensity of the slow mode A_3, for the 8% copolymer solution measured at $\theta=90°$.

This interpretation of the slow mode is also supported by the macroscopic phase separation observations discussed earlier. We observed that samples prepared at concentrations $c=2$, 4 and 6% split into two sharply separated phases in several days: (1) a liquid phase with a low light scattering intensity and (2) a gel phase with low turbidity. The copolymer concentration of the equilibrated gel phase evaluated from the three samples was $c_e=7.5\pm0.2\%$. Zero-angle limits of Γ_i for the gel phase of the sample with $c=6\%$ shown for comparison in Table 2 are close to those observed for sample with $c=8\%$ at room temperature. The sample with $c=8\%$ is close to the equilibrium concentration of the physical gel, and has minimal microsynerisis. This may explain the low turbidity of freshly made samples at this concentration and their stability with time.

3.4. Comparison of the association behavior with similar systems

To examine the influence of varying solvent selectivity on the association behavior we compare the SANS and DLS results described above with those obtained previously from the same pentablock in 1,4-dioxane [19]. As shown in the inset of Fig. 2, a 7% solution of the same pentablock in 1,4-dioxane shows very weak association behavior [19] with less than 10% volume fraction of hard spheres at room temperature. Moreover, the 4% solution in *n*-heptane still

exhibits a scattering peak, which is completely absent in the scattering pattern of the 4% solution of the same pentablock in 1,4-dioxane [19]. The aggregation numbers are more than one order of magnitude higher in *n*-heptane than those in dioxane solutions of the same pentablocks [19]. DLS results show that the pentablock does not form a gel in dioxane, even up to 22%, but only forms large aggregates. The relaxational dynamics of the insoluble domains (Γ_2) is not observed in dioxane; instead a diffusive mode corresponding to the diffusion of large aggregates is observed.

The increased association in *n*-heptane as compared to dioxane can be related to the solvent selectivity. Using the values of solubility parameters of polystyrene, polybutadiene and *n*-heptane ($\delta_{PS}=18.6$, $\delta_{PB}=17.2$, $\delta_{heptane}=15.1$ $(10^3[J/m^3]^{1/2})$, and the molar volume of *n*-heptane as 146.5 cm^{-3}), we get the enthalpic contribution χ_H of the two polymers in *n*-heptane as $\chi_{heptane,\,PB}\sim 216/T$ which is significantly higher than $\chi_{heptane,\,PS}\sim 77/T$. In contrast, dioxane, a theta solvent for PB at 26.5 °C, is only slightly selective for PS ($\chi_{dioxane,\,PB}\sim 33/T$). Using the total number of monomers of the insoluble blocks, we estimate that the enthalpic contribution of the three insoluble PS blocks in *n*-heptane solutions is stronger than that of the two insoluble PB blocks in dioxane solutions (by a factor of about 2). Entropic effects of bridging versus looping will also be larger in heptane as compared to dioxane. Another factor which may be involved is the solubility of the outermost blocks. The outer PS blocks are in a good solvent environment in dioxane leading to the formation of aggregates, whereas the outer PS blocks are in a poor solvent environment in *n*-heptane leading to gelation.

A comparison of the pentablock in heptane with that of a very similar triblock S-EB-S in heptane [26] may be related to the effect of increasing number of blocks. The two polymers have comparable overall molecular weights (around 120,000 g/mole for the pentablock as compared to 100,000 g/mole for the triblock), similar molecular weights of the insoluble PS blocks $(0.9–1.3)\times 10^4$ g/mole) and weight fraction of styrene (28 vs 35% for SEBS vs SBSBS). However, it is important to note that the two polymers differ in solubility of the middle block (EB in the triblock is slightly better soluble in heptane than butadiene) and the single PEB block in SEBS is longer than each of the two PB blocks in SBSBS. With these qualifications, we note that the core radius of around 8 nm and aggregation numbers around 185 in a 7% sample of SEBS at 25 °C [33] is comparable to that of the pentablock which showed 10 nm cores with slightly larger aggregation numbers. However, the temperature dependence differed in the two samples: the SANS peak started to decrease at 40 °C in the triblock [12] but still persisted in the pentablock at least up to 60 °C suggests that increasing number of blocks increases the stability of the multiplet domains. This difference also shows up in the temperature dependence of the middle mode in the DLS which remains relaxational at all temperatures in the pentablock while it changes to diffusive again at 40 °C in the triblock. The pentablock exhibits strong microsynerisis, shows macroscopic phase separation and does not form flower-like micelles unlike the similar triblock. Thus the starting situation for gelation in pentablocks is likely to be different than those in equivalent triblocks which form gels by bridging micellar cores. These differences suggest that the pentablock forms physical gels by bridging of multiplets, similar to the prediction of Nyrkova et al [16] for multiblock copolymer melts. The cooperative effect of the bridging of three crosslinking domains in the pentablock as compared to only two in the triblock perhaps make the pentablock's behavior closer to physical gels where a single chain participates in multiple crosslinks.

4. Conclusions

We have examined dilute and semidilute solutions of a poly(SBSBS) pentablock copolymer in *n*-heptane, a strongly selective solvent for the PB blocks, using static and dynamic light scattering and small angle neutron scattering. The SANS data clearly indicate the presence of interacting domains of about 10 nm radius formed by association of about 200 of the insoluble PS blocks. The volume fraction and size of micro-domains decreased as temperature was increased up to 80 °C, but they did not dissolve over this temperature range. The DLS data provide further support that this association behavior is related to the differing solubility of the two components and shows three modes. The fast diffusive mode corresponds to the cooperative mode of the concentration fluctuations in the gel, and the intermediate relaxational mode reflects the local dynamics of domains of the insoluble blocks (multiplets) trapped in the network of the physical gel. The formation of multiplet domains is similar to that predicted for multiblock copolymer melts and ionomers. The slow diffusive mode is the most difficult to interpret. Its strong temperature dependence suggests that it may be related to microsynerisis. The pentablock copolymer has a limited range of solubility in heptane which shows up in a cloud point at 57 °C in a dilute unassociated solution. No flower-like micelles were observed in dilute solutions above 57 °C. At higher concentrations we were able to observe a macroscopic phase separation into a liquid and a gel phase, suggesting that the interplay of phase separation and physical gelation could lead to microsyneresis in these systems.

Acknowledgements

R.B. acknowledges the support of NSF-Div. of Materials Research (NSF-DMR No. 9618467 including International Supplement). C.K. acknowledges the financial support of the Alexander von Humboldt Foundation, the Grant Agency

of the Academy of Sciences (A1050201 and A4050305) and the Grant Agency of the Czech Republic (No. 203/03/0600).

References

[1] Hamley IW. The physics of block copolymers, 1st ed. New York: Oxford University Press; 1998.
[2] Tuzar Z, Kratochvíl P. In: Matijevic E, editor. Surface and colloid science series. New York: Plenum Press; 1993. p. 1.
[3] Riess G, Hurtrez G, Bahadur P. In: Mark H, Bikales NM, Overberg CG, Menges G, editors. Encyclopedia of polymer sciences and engineering, vol. 2. New York: Wiley; 1982. p. 234.
[4] Hanley KJ, Lodge TP. Macromolecules 2000;33:5918–31.
[5] Lodge TP, Pudil B, Hanley KJ. Macromolecules 2002;35:4707–17.
[6] Lairez D, Adam M, Carton JP, Raspaud E. Macromolecules 1997;30: 6798–809.
[7] Euzar Z, Koňák Č, Šteăpánek P, Pleštil J, Kratochvíl P, Procházka K. Polymer 1990;31:2118–24.
[8] Pleštil J, Hlavatá D, Hrouz J, Tuzar Z. Polymer 1990;31:2112–7.
[9] Balsara NP, Tirrell M, Lodge TP. Macromolecules 1991;24:1975–86.
[10] Kleppinger R, Mischenko N, Reynaers HL, Koch MHJ. J Polym Sci, Part B: Polym Phys 1999;37:1833–40.
[11] Laurer JH, Mulling JF, Khan SA, Spontak RJ, Bukovnic R. J Polym Sci, Part B: Polym Phys 1998;(36):2379–91.
[12] Bansil R, Nie H, Li Y, Liao G, Ludwig K, Steinhart M, Koňák Č, Lal J. Macromol Symp 2002;190:161.
[13] Nie H, Bansil R, Ludwig K, Steinhart M, Koňák Č, Bang J. Macromolecules 2003;36:8097.
[14] Glatter O, Scherf G, Schillen K, Brown W. Macromolecules 1994;27: 6046–54.
[15] Hamley IW, Fariclough JPA, Ryan AJ, Ryu CY, Lodge TP, Gleeson AJ, Pedersen JS. Macromolecules 1998;31:1188–96.
[16] Nyrkova IA, Khokhlov AR, Doi M. Maromolecules 1993;26: 3601–10.
[17] Burchard W. Trends Polym Sci 1993;1:192–8.
[18] Glotzer SC, Bansil R, Gallagher P, Gyure MF, Sciortino F, Stanley HE. Physica A 1993;201:482–95.
[19] Bansil R, Nie H, Koňák Č, Helstedt M, Lal J. J Polym Sci: Part B 2002;40:2807.
[20] Jakeš J. Collect Czech Chem Commun 1995;60:1781.
[21] Provencher SW. Comput Phys Commun 1982;27:229.
[22] Thiyagarajan P, Epperson JE, Crawford RK, Carpenter JM, Klippert TE, Wozniak DG. J Appl Crystallogr 1997;20:280.
[23] Kinning DJ, Thomas EL. Macromolecules 1984;17:1712–8.
[24] Bansil R, Lal J, Carvalho BL. Polymer 1992;33:2961–9.
[25] Stejskal J, Hlavatá D, Sikora A, Koňák Č, Pleštil J, Karatocvíl P. Polymer 1992;33:3675.
[26] Koňák Č, Fleischer G, Tuzar Z, Bansil R. J Polym Sci: Part B: Polym Phys 2000;38:1312.
[27] Fleischer G, Koňák Č, Puhlmann A, Rittig F, Kärger J. Macromolecules 2000;33:7066.
[28] Koňák M, Koňák Č, Bansil R. Physica A 1991;171:19.
[29] Kanaya T, Patkowski A, Fischer EW, Seils J, Glaser H, Kaji K. Acta Polym 1994;45:137.
[30] Heckmeier M, Mix M, Strobl G. Macromolecules 1997;30:4454–8.
[31] Šteăpánek P, Lodge TP. Macromolecules 1996;29:1244–51.
[32] Vogt S, Anastasiadias SH, Fytas G, Fischer EW. Macromolecules 1994;27:4335–43.
[33] Liao G. Kinetics of phase transitions in polymers, PhD Thesis, Boston University; 1998.